Received: 16 July 2017 | Revised: 30 August 2017 | Accepted: 8 September 2017

DOI: 10.1002/er.3907

RESEARCH ARTICLE

WILEY INTERNATIONAL JOURNAL OF ENERGY RESEARCH

Effect of high irradiation on photovoltaic power and energy

R. Nasrin[1,2] | M. Hasanuzzaman[1] | N.A. Rahim[1,3]

[1] UM Power Energy Dedicated Advanced Centre (UMPEDAC), Level 4, Wisma R&D, University of Malaya, 59990 Kuala Lumpur, Malaysia

[2] Department of Mathematics, Bangladesh University of Engineering and Technology, Dhaka 1000, Bangladesh

[3] Renewable Energy Research Group, King Abdulaziz University, Jeddah 21589, Saudi Arabia

Correspondence
R. Nasrin, Department of Mathematics, Bangladesh University of Engineering and Technology, Dhaka 1000, Bangladesh.
Email: rehena@math.buet.ac.bd

Funding information
UMPEDAC, Higher Institution Center of Excellence (HICoE) Grant, Ministry of Higher Education, Malaysia, Grant/Award Number: UM.0000067/HME.OM, UMPEDAC - 2016

Summary

Solar photovoltaics (PV) is a promising solution to combat against energy crisis and environmental pollution. However, the high manufacturing cost of solar cells along with the huge area required for well-sized PV power plants are the two major issues for the sustainable expansion of this technology. Concentrator technology is one of the solutions of the abovementioned problem. As concentrating the solar radiation over a single cell is now a proven technology, so attempt has been made in this article to extend this concept over PV module. High irradiation intensity from 1000 to 3000 W/m^2 has been investigated to measure the power and energy of PV cell. The numerical simulation has been conducted using finite element technique. At 3000 W/m^2 irradiation, the electrical power increases by about 190 W compared with 63 W at irradiation level of 1000 W/m^2. At the same time, at 3000 W/m^2 irradiation, the thermal energy increases by about 996 W compared with 362 W at 1000 W/m^2 irradiation. Electrical power and thermal energy are enhanced by about 6.4 and 31.3 W, respectively, for each 100-W/m^2 increase of solar radiation. The overall energy is increased by about 179.06% with increasing irradiation level from 1000 to 3000 W/m^2. It is concluded that the effect of high solar radiation using concentrator can significantly improve the overall output of the PV module.

KEYWORDS
energy, high irradiation, power, PV cell

1 | INTRODUCTION

Energy is one of the key factors of economic growth as well as social development where the energy demand increases globally. Renewable energies are taken into account and being paid attention to fulfill the energy demand and environmental concerns. Among the renewable energy sources, the photovoltaic (PV) system is a high potential, effective, and sustainable system. However, in operation, electrical power about 15 to 20% and thermal energy about 75 to 80% may be generated from incident solar radiation.[1,2] The converted heat overheats

Nomenclature: A, = total area of photovoltaic (PV) solar cell (m^2); C_p, = specific heat (J kg^{-1} K^{-1}); E_p, = module's electrical power (W); E_{in}, = received energy by solar cell (W); E_t, = thermal energy in the system (W); E_l, = lost energy from glass layer to ambient (W); G, = solar irradiance (W m^{-2}); k, = thermal conductivity (W m^{-1} K^{-1}); T_{amb}, = ambient temperature (°C); T_f, = water temperature (°C); T_g, = glass temperature (°C); T_{he}, = heat exchanger temperature (°C); T_{in}, = inlet temperature (°C); T_{out}, = outlet temperature (°C); T_r, = reference temperature (°C); T_s, = side boundary temperature (°C); T_{sc}, = cell temperature (°C); T_{td}, = Tedlar temperature (°C); U_{he}, = heat loss coefficient from back surface to air (W m^{-2} K^{-1}); U_{sca}, = heat loss coefficient from glass to air (W m^{-2} K^{-1}); U_t, = heat transfer coefficient inside photovoltaic/thermal (PVT) surfaces (W m^{-2} K^{-1}); V_{in}, = input velocity of water (m s^{-1}) **Greek symbols:** α_g, = glass absorptivity; α_{sc}, = PVT module absorptivity; τ_g, = transmitivity of glass; ε_g, = emissivity of glass; ρ, = density (kg m^{-3}); μ_{sc}, = thermal coefficient of cell efficiency (%/°C); η_{sc}, = reference electrical efficiency of PV cell; η_e, = PV electrical efficiency; η_t, = PVT efficiency; η_{tot}, = PVT overall efficiency

the PV system and reduces its efficiency. Thus, the photovoltaic/thermal (PVT) system is more effective because it collects extra heat for maintaining cell temperature to achieve better electrical efficiency as well as uses the thermal energy. Generally, a heat exchanger is attached to the PV Tedlar surface, and air/water is considered as cooling fluids to collect heat from this system.[3]

The extracted heat from the PVT system can be used for space heating, building ventilation, agricultural, industrial materials drying, etc.[4,5] Numerical and experimental researches[6,7] have been conducted with various designs of PVT. Solar thermal collectors along with PV module make a combined form of the PVT system.[8-10] Nowadays, system design and operational factors are the main focus points to increase electrical and thermal efficiencies and to reveal the potential of this PVT system.[11-17] The performance of the PV/PVT also depends on climatic conditions.[18,19] For Malaysia's climate condition, the performance of amorphous silicon PV cell is found better.[20] Actual data were analyzed for more than 6 years' period in Gobi Desert area in Mongolia, and it was found that the crystalline silicon PV cell performs better.[21]

The crucial role is played by operating temperature in the PV system even at the situation of other well controlled factors. Operating temperature affects the performance of the PV module. The PV module's output power and efficiency reduce if the cell temperature increases.[22-26] The authors also showed that electrical efficiency decreased by 0.469% for the increase of each degree Celsius of solar cell temperature. The authors investigated 13 different types of PV modules in Stuttgart, Germany and Nicosia, Cyprus and found that the variation of temperature coefficient are −0.039%/°C to −0.461%/°C, −0.403%/°C to −0.502%/°C, and −0.353%/°C to −0.456%/°C for amorphous silicon, multicrystalline, and monocrystalline PV cells, respectively. The efficiency decreases by 0.25%/°C and 0.45%/°C for PV module with amorphous cells and both polycrystalline and monocrystalline cells, respectively. In Japan, there was a PV system of 50-kW setup to analyze field test data,[27] and it was found that high operative temperature affects PV module's performance. About 1% increment of annual output energy is observed for 0.1%/°C increment of the temperature coefficient because of the effect of temperature coefficient on conversion efficiency. By using the front side glass cover and back Tedlar white insulating material, the cell temperature rises because of unused solar energy in cells and received energy by the gap between 2 cells. In this opaque PV module, bottom Tedlar heat loss is found to be lower than semitransparent PV module.[28,29] The performance of PV module depends on temperature, and at higher temperatures, PV modules lose up to 7% power.[30]

Because of the greater reduction in voltage, the output power of PV module diminishes with increased temperature. It is also essential to investigate the solar intensity effect on temperature. PV power increases with solar intensity, but the efficiency tends to decrease because of cell temperature. Recently, converging lenses are used as solar concentrator, and microprocessor is used to control concentrator's position for increasing PV overall performance.[31-33] The authors used silicon solar cell as well as multijunction solar cell for PV module and analyzed the economical feasibility as well. Experimental and numerical researches were performed[34-40] based on PVT performance, system of pyramid-shaped solar water purification, solar collector of flat plate pattern, mini channel–based solar collector, evacuated tube, etc. The authors used different water-based nanofluids as well as water as heat transfer medium to enhance the thermal performance of the systems and reviewed the application of nanofluids on solar energy. Indoor experiment and numerical technique were implemented to measure the performance of different types of solar cells with/without nano-coating, thermal management of PVT system, and economical feasibility of clean energy technology.[41-44] For this purpose, the authors used multijunction solar cell, electrical battery–based vehicles, and pipe plate–based PVT.

From the above literature, it is apparent that PV technology is one of the best way to achieve clean and sustainable energy goal[41-44] if the power density and efficiency can be improved further. However, conventional PV systems possess very low efficiency and low power density, which dictates to shift for concentration. However, there is a very limited research (experimental and numerical) based on traditional PV module using concentrator to optimize the use of PV module's electric and thermal energy at high irradiation. Using the lens panel, the focus of high irradiation on PV system is economically feasible because of lower price of the lens than the solar cell. The aims of the present research are to simulate the heat transfer model in each layer of PV module coupling with the fluid flow model in details using 3-dimensional FEM-based Comsol Multyphysics software; investigate the high irradiation effect on PV temperature and electrical-thermal-overall efficiencies; and evaluate the PVT outcomes in terms of power and energy.

2 | METHODOLOGY

2.1 | Experimental investigation

The outdoor experimental investigation has been conducted in Solar Garden, Level 3, UMPEDAC, UM, KL, Malaysia. It was performed to collect solar cell

temperature for low irradiation up to 1000 W/m^2. The SY-90M monocrystalline module is used for this experiment. Details of this experimental setup, experimental instruments, operating conditions, and SY-90M PV module's specifications are given in Rahman et al.[2] Data are taken in the month of January 2017. Figure 1 displays the experimental setup.

The collected data are analyzed to find the relation between irradiation and PV temperature. Table 1 expresses the irradiation against solar cell temperature, which is calculated using Equation 7.

A correlation is developed by using experimental results (Table 1) between PV cell temperature (T_{sc}) and solar radiation (G). The correlation can be written as

$$T_{sc} = 2.4308^{*}(G)^{0.4352} \text{ where the correlation coefficient is } r^2 = 0.9741. \quad (1)$$

This correlation is used to conduct numerical investigation for finding the PV performance due to high irradiation (G) up to 3000 W/m^2.

There is a relation[31] between lens area (A_l) and cell area (A) in order to find the concentration ratio (C_r): $C_r = A_l/A$.

Normally in Malaysia, average solar radiance is 1000 W/m^2. To get 3000 W/m^2 irradiation, each lens area becomes 3 times of each solar cell area.

2.2 | Development of the model

The idea of concentrating solar irradiation has been exaggerated from cell to module level in this research. That is, each and every cell of PV module receives concentrated solar energy from the individual concentrating lens. The schematic of the PV module with concentrator is shown in the form of the magnified view in Figure 2A, full view in Figure 2B, and cross-sectional view of the PVT in Figure 2C. A converging lens panel consisting of 36

TABLE 1 Solar cell temperature for various irradiation

Irradiation G (W/m^2)	Solar cell temperature T_{sc} (°C)
300	30.6
351	31.76
362	31.93
395	32.77
442	33.99
469	35.25
585	36.79
622	38.14
688	39.55
702	40.95
708	41.96
717	42.14
738	42.79
771	43.91
830	45.13
849	46.91
871	47.35
904	48.11
957	48.63
967	49.01
973	49.33
983	49.76
994	49.99

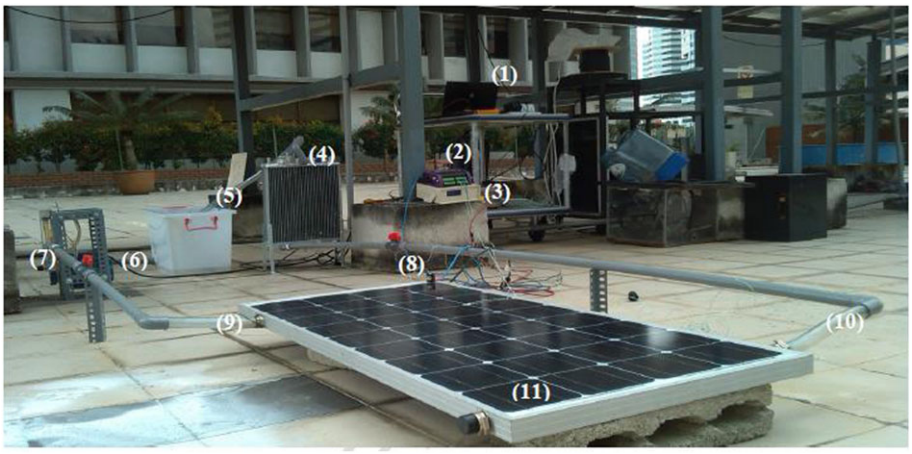

FIGURE 1 Experimental setup where (1) monitor, (2) dataTaker, (3) MPPT, (4) radiator, (5) water tank, (6) pump, (7) flow meter, (8) pyranometer, (9) water inlet, (10) water outlet, and (11) PV module [Colour figure can be viewed at wileyonlinelibrary.com]

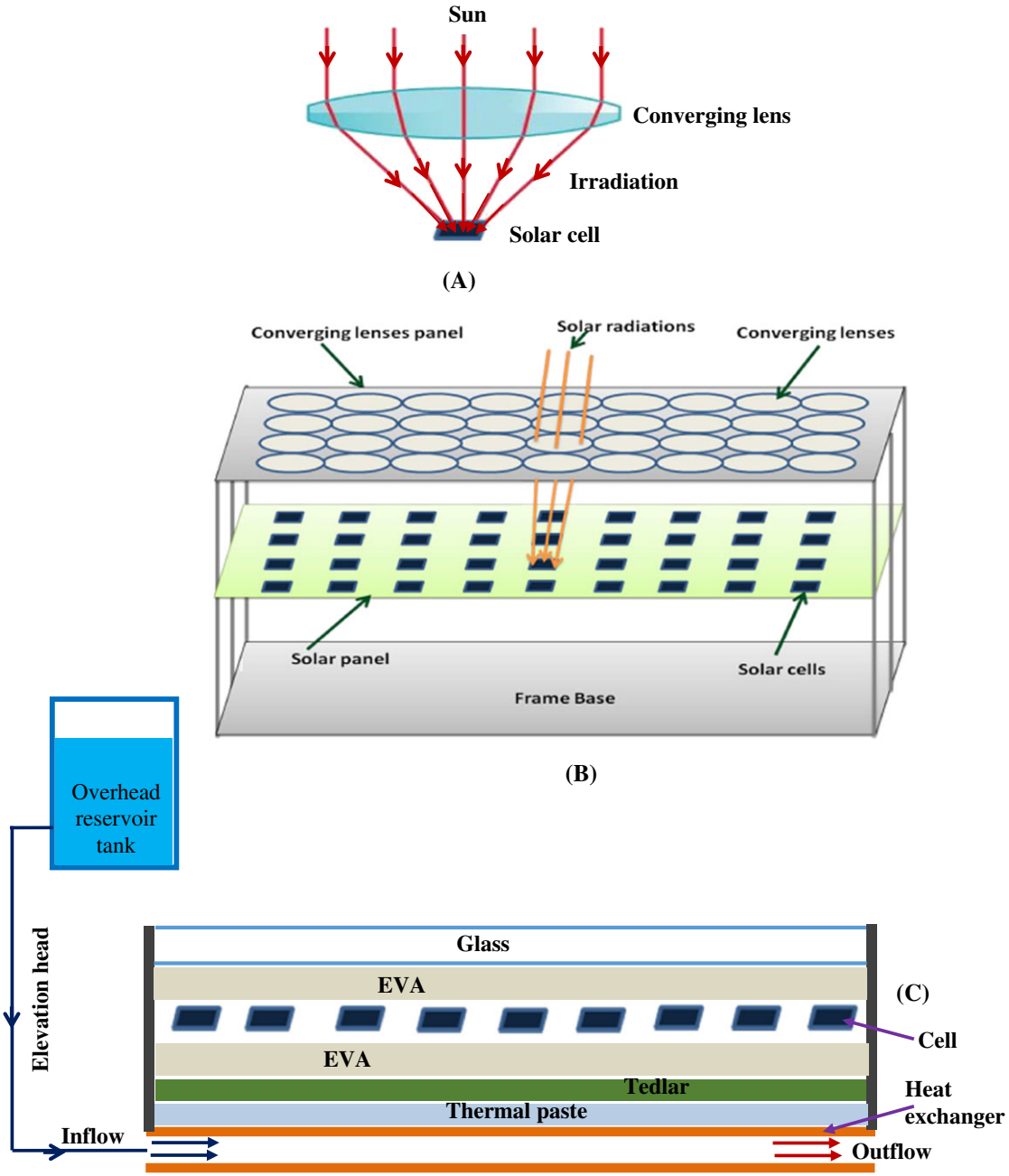

FIGURE 2 Schematic diagram of (A) the magnified view of Fresnel lens with cell, (B) the arrangement of lens panel with solar panel, and (C) the cross-sectional view of the PV module with cooling system [Colour figure can be viewed at wileyonlinelibrary.com]

Fresnel lenses is used to concentrate the sunlight to each of the solar cells of a 36-cell monocrystalline PV module. In order to get higher irradiation from 1000 to 3000 W/m^2, focal length of the lenses may be adjusted through mechanical or electrical adjustment mechanism. The monocrystalline solar cells with conventional ethyl vinyl acetate (EVA) lamination on both sides and polyvinyl fluoride or Tedlar coating on the back side are arranged so that each cell surface becomes the focal part of the lens. Therefore, the structure of PV modules is different from that of the conventional ones where the packing factor is lower than that of traditional PV module. For cooling purpose, a box-shaped heat exchanger of aluminum metal has been attached by using thermal paste to the PV bottom surface. Inlet and outlet ports of square form (10 × 10 mm) having the same material are attached with the heat exchanger. Water is considered as heat transfer fluid. Inlet fluid flows because of the overhead reservoir tank as shown in Figure 2C. Heat is transferred from PV layers to cooling fluid mainly by natural convection process. Properties of different materials of the PVT system are expressed in Table 2.

The physical dimension and properties of different layers of PV module are expressed in Table 3.

TABLE 2 PV module's properties[2,45]

Properties	Value
Glass transmissivity, τ_g	0.96
Emissivity of glass, ε_g	0.04
Solar cell absorptivity, α_{sc}	0.9
Tedlar absorptivity, α_b	0.95
Heat transfer coefficient from glass to air	7.14
Heat transfer coefficient inside PVT surfaces	150
Heat loss coefficient from back surface to air	6
Reference efficiency of cell, η_{sc}	0.13
Thermal coefficient of PV cell efficiency, μ_{sc} (%/°C)	−0.0045
Reference temperature, T_r (°C)	25
Number of cells	4 × 9
Area of each cell (m^2)	0.125 × 0.125
Ambient temperature, T_{amb} (°C)	32
Fluid input temperature, T_{in} (°C)	30

2.3 | Mathematical formulation

The amount of total received energy by the solar cell of the PVT module is calculated as[2]

$$E_{in} = \tau_g \alpha_{sc} GA \tag{2}$$

By the convection process, some part of this energy goes to the ambient air through glass, which is

$$E_l = U_{sca}(T_{sc} - T_{amb})A \tag{3}$$

Electrical power is generated from some part of the rest energy:

$$E_e = \eta_{sc} GA \tag{4}$$

The rest energy transfers by heat conduction procedure as thermal energy. Thus, the total useful thermal energy in the PVT system is

$$E_t = U_t(T_{sc} - T_{he})A \tag{5}$$

So, the PV module's energy conservation equation is

$$E_{in} = E_l + E_t + E_e \tag{6}$$

The solar cell temperature[2] is obtained from Equation 6:

$$T_{sc} = \frac{G(\tau_g \alpha_{sc} - \eta_{sc}) + (U_{sca} T_a + U_t T_{he})}{(U_{sca} + U_t)} \tag{7}$$

The 3D numerical simulation has performed in steady-state conditions. Transmitivity of EVA is about 100%; no dust on PV surface may affect solar energy absorptivity. The flow is considered to be laminar and incompressible; thermal-physical properties of the heat exchanger are constant with respect to the operating temperature; and negligible amount of temperature varies along thickness. The leading partial differential equations in the form of thermal energy equations for PV solid layers as well as fluid layer, continuity and momentum equations for fluid layer are given below[9]:

For the solid layers

$$-\left(\frac{k}{\rho C_p}\right)\left(\frac{\partial^2 T}{\partial x^2} + \frac{\partial^2 T}{\partial y^2} + \frac{\partial^2 T}{\partial z^2}\right) = 0 \tag{8}$$

For the fluid layer

$$\frac{\partial u}{\partial x} + \frac{\partial v}{\partial y} + \frac{\partial w}{\partial z} = 0 \tag{9}$$

$$\rho_f\left(u\frac{\partial u}{\partial x} + v\frac{\partial u}{\partial y} + w\frac{\partial u}{\partial z}\right) = -\frac{\partial p}{\partial x} + \mu_f\left(\frac{\partial^2 u}{\partial x^2} + \frac{\partial^2 u}{\partial y^2} + \frac{\partial^2 u}{\partial z^2}\right)$$
$$\Rightarrow\left(u\frac{\partial u}{\partial x} + v\frac{\partial u}{\partial y} + w\frac{\partial u}{\partial z}\right) = -\frac{1}{\rho_f}\frac{\partial p}{\partial x} + \frac{1}{\mathrm{Re}}V_{in}D_h\left(\frac{\partial^2 u}{\partial x^2} + \frac{\partial^2 u}{\partial y^2} + \frac{\partial^2 u}{\partial z^2}\right) \tag{10}$$

TABLE 3 Physical properties and dimensions of PVT surfaces[2,45]

Surfaces	Thickness (m)	Thermal conductivity k (W/mK)	Density ρ (kg/m^3)	Specific heat C_p (J/kg K)
Glass	0.003	1.8	3000	500
Monocrystalline cell	225×10^{-6}	148	2329	700
EVA	500×10^{-6}	0.311	950	2090
Tedlar	0.0001	0.15	1200	1250
Thermal paste	0.0003	1.9	2600	700
Heat exchanger	0.001	2700	237	900
Inflow and outflow pipes	0.01(inner diameter)	2700	237	900
Water	0.01 (fluid region)	0.68	998	4200

$$\rho_f\left(u\frac{\partial v}{\partial x}+v\frac{\partial v}{\partial y}+w\frac{\partial v}{\partial z}\right)=-\frac{\partial p}{\partial y}+\mu_f\left(\frac{\partial^2 v}{\partial x^2}+\frac{\partial^2 v}{\partial y^2}+\frac{\partial^2 v}{\partial z^2}\right)$$
$$\Rightarrow\left(u\frac{\partial v}{\partial x}+v\frac{\partial v}{\partial y}+w\frac{\partial v}{\partial z}\right)=-\frac{1}{\rho_f}\frac{\partial p}{\partial y}+\frac{1}{\mathrm{Re}}V_{in}D_h\left(\frac{\partial^2 v}{\partial x^2}+\frac{\partial^2 v}{\partial y^2}+\frac{\partial^2 v}{\partial z^2}\right) \quad (11)$$

$$\rho_f\left(u\frac{\partial w}{\partial x}+v\frac{\partial w}{\partial y}+w\frac{\partial w}{\partial z}\right)=-\frac{\partial p}{\partial z}+\mu_f\left(\frac{\partial^2 w}{\partial x^2}+\frac{\partial^2 w}{\partial y^2}+\frac{\partial^2 w}{\partial z^2}\right)$$
$$\Rightarrow\left(u\frac{\partial w}{\partial x}+v\frac{\partial w}{\partial y}+w\frac{\partial w}{\partial z}\right)=-\frac{1}{\rho_f}\frac{\partial p}{\partial z}+\frac{1}{\mathrm{Re}}V_{in}D_h\left(\frac{\partial^2 w}{\partial x^2}+\frac{\partial^2 w}{\partial y^2}+\frac{\partial^2 w}{\partial z^2}\right) \quad (12)$$

$$(\rho_f C_{pf})\left(u\frac{\partial T_f}{\partial x}+v\frac{\partial T_f}{\partial y}+w\frac{\partial T_f}{\partial z}\right)=k_f\left(\frac{\partial^2 T_f}{\partial x^2}+\frac{\partial^2 T_f}{\partial y^2}+\frac{\partial^2 T_f}{\partial z^2}\right)$$
$$\Rightarrow\left(u\frac{\partial T_f}{\partial x}+v\frac{\partial T_f}{\partial y}+w\frac{\partial T_f}{\partial z}\right)=\frac{1}{Re\ \ Pr}V_{in}D_h\left(\frac{\partial^2 T_f}{\partial x^2}+\frac{\partial^2 T_f}{\partial y^2}+\frac{\partial^2 T_f}{\partial z^2}\right) \quad (13)$$

Here let $\mathrm{Pr}=\frac{\mu_f C_{pf}}{k_f}$ be the Prandtl number and $\mathrm{Re}=\frac{V_{in}D_h\rho_f}{\mu_f}$ be the Reynolds number where D_h be the hydraulic diameter that is defined as $D_h=\frac{4A_{in}}{p_{in}}$. Here A_{in}, p_{in}, V_{in}, μ_f, k_f, ρ_f, and C_{pf} are the cross-sectional area of inlet boundary, perimeter of the inlet pipe, inlet fluid velocity, dynamic viscosity, thermal conductivity, density, and specific heat at constant pressure of cooling water, respectively.

2.3.1 | Boundary conditions

1. At the top surface of the PV: inward heat flux $-k_g\frac{\partial T_g}{\partial z}=G$
2. At the top surface of the PV: diffuse surface condition $-\mathbf{n}\cdot q=\varepsilon\sigma\left(T_{amb}^4-T_g^4\right)$, where σ (= 5.670 367 × 10^{-8} W m^{-2} K^{-4}) is the Stefan-Boltzmann constant
3. At the top surface of the PV: convective heat loss $-\mathbf{n}\cdot q=U_{sca}(T_{amb}-T_g)$
4. At the outer boundaries of inflow and outflow pipes, bottom boundary of heat exchanger: convective heat loss condition $-\mathbf{n}\cdot q=U_{he}(T_{amb}-T_{he})$
5. At the side boundaries of PVT module: insulation $\frac{\partial T_s}{\partial n}=0$
6. At all solid boundaries of the fluid passing path: no-slip condition $u=v=w=0$
7. At the solid-fluid interface inside heat exchanger: $k_f\left(\frac{\partial T}{\partial n}\right)_f=k_{he}\left(\frac{\partial T}{\partial n}\right)_{he}$
8. At the inlet: $u=0$, $v=V_{in}$, $w=0$, and $T=T_{in}$
9. At the outlet: $p=0$

where n be the surface normal distance along the x- or y- or z-axis, respectively.

2.3.2 | Electrical power

The following equation[45] gives the output electrical power of the PV:

$$E_p=\eta_{sc}\tau_g\alpha_{sc}GA[1-\mu_{sc}(T_{sc}-T_r)] \quad (14)$$

2.3.3 | Thermal energy

Using the following relation, the output thermal energy of the PV module can be measured[9]:

$E_t=mC_{pf}(T_{out}-T_{in})$, where

$$m=\rho_f V_{in}A_{in} \quad (15)$$

is the mass flow rate.

2.3.4 | Efficiency

The instantaneous PV module's electrical efficiency is[45]

$$\eta_e=\frac{\text{Produced electrical power}}{\text{Total received energy}}=\frac{E_p}{E_{in}} \quad (16)$$

and thermal efficiency of PVT module is[9]

$$\eta_t=\frac{\text{Extracted thermal energy}}{\text{Total received energy}}=\frac{E_t}{E_{in}} \quad (17)$$

Overall efficiency can be determined by[45]

$$\eta_{tot}=\frac{E_p+E_t}{E_{in}} \quad (18)$$

2.4 | Numerical technique

The COMSOL Multiphysics software based on FEM is used to solve the 3D numerical model. The finite element technique[46] is applied for solving Equations 8 to 13 for this numerical simulation. To know the temperature (T_{sc}, T_{out}) distribution of solar cell inside the PV module, the energy conservation equations play a very important role. The details in numerical technique are described in Nasrin and Alim[47] and are not repeated in this section.

2.4.1 | Mesh generation and grid check

Figure 3 expresses the meshing of PVT system computational area. For this numerical simulation, normal type meshing is considered from the built-in-physics–controlled mesh sequence in COMSOL Multiphysics. Free tetrahedral and free triangular elements are used in subdomains and the boundaries of the numerical model, respectively. In addition, different types of mesh elements like pyramid, prism, and quadrilateral are also observed in the model. A grid-independent check for the PVT module is performed at $G = 1000$ W/m^2 with volume flow rate 180 L/h. Nonuniform grid systems consisting elements 103 560; 174 938; 432 674; 718 898; and 1 947 577 are tested. Temperature of solar cell (T_{sc}) is assumed as the controlling parameter. No significant change in cell temperature's value is obtained for fine type of meshing in Table 4. On the other hand more time is needed for required simulation in COMSOL Multiphysics. Thus, 718,898 domain elements (boundary elements 169 731 and edge elements 4406) are considered for numerical analysis. This normal-type meshing

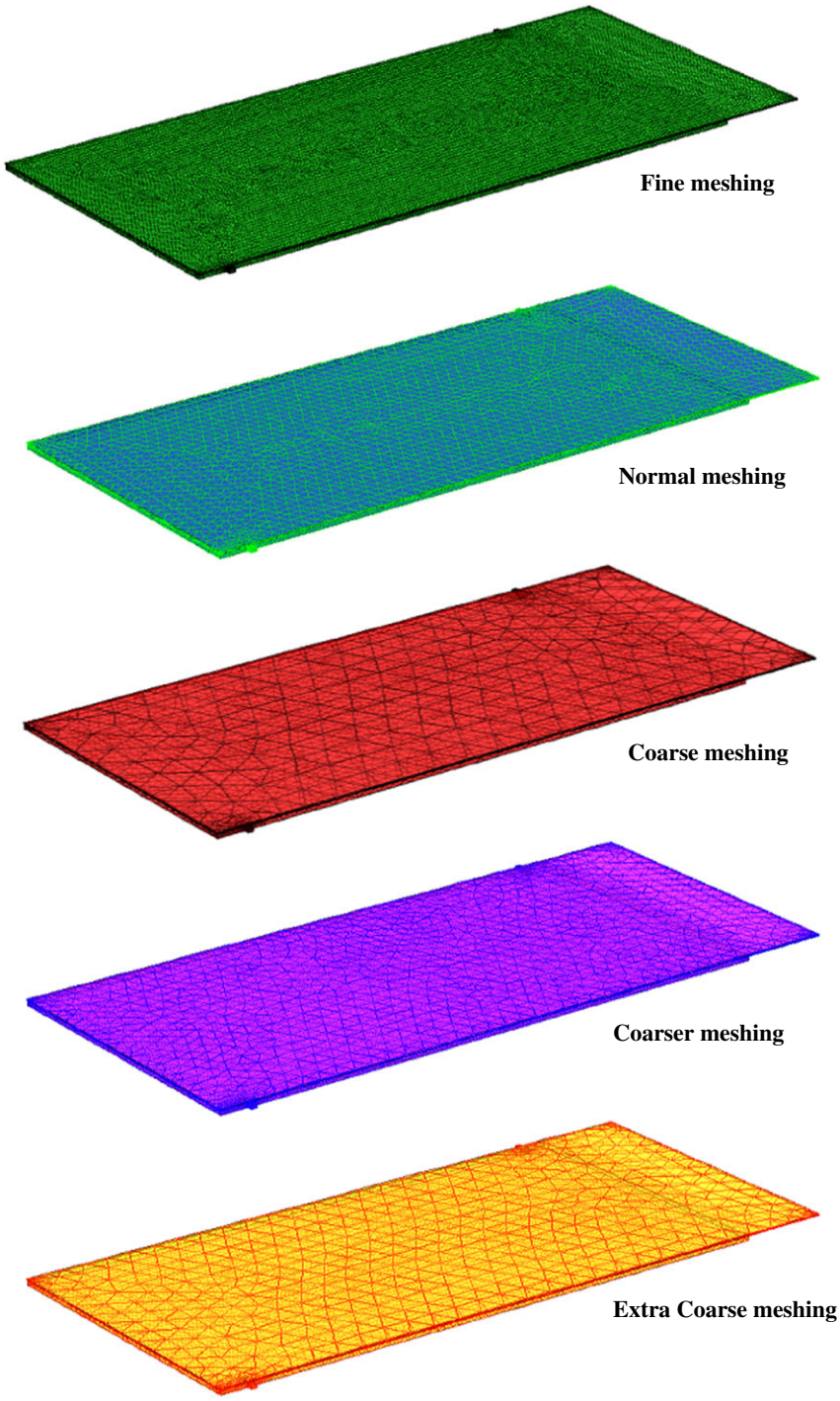

FIGURE 3 Different types of meshing of PVT module [Colour figure can be viewed at wileyonlinelibrary.com]

TABLE 4 Grid sensitivity check at $G = 1000$ W/m^2

Type of meshing	Extra Coarse	Coarser	Coarse	Normal	Fine
Elements	103 560	174 938	432 674	**718 898**	1 947 577
Cell temperature (°C)	46.305 35	46.912 48	47.427 51	**48.010 12**	48.010 21
Time of solution (s)	98	193	287	**405**	979

consists of 181 376 vertices, 264 pyramid elements, 152 160 prism elements, 444 quadrilateral elements, and 74 vertex elements.

2.4.2 | Model validation

The current 3D numerical simulation of PV module has been validated with both experimental result and numerical result. These are given as follows:

Validation with experimental result

The current numerical result is compared for solar cell temperature (T_{sc}) at the 5 different irradiation level $G = (397, 587, 704, 852$ and 997 W/m^2) for the PVT system with that of Rahman et al.[2] They studied the effects of operating conditions in PV modules in Malaysia. The effects of irradiation, flow rate of cooling fluid (water), cell temperature, humidity, and dust were investigated in their study. The authors[2] used the SY-90M PV module of monocrystalline cells for experimental purpose. The operating temperature was −40 to 75°C, and volume flow rate was 90 L/h. The validation is displayed in Table 5 including percentages of error. Numerical result agrees well with Rahman et al.[2] So this numerical model can produce valid results to analyze the PV performance.

TABLE 5 Model validation of solar cell temperature of PVT against irradiation

Solar Irradiance G (W/m^2)	Solar Cell Temperature T_{sc} (°C)		Percentage of Error (%)
	Rahman et al[2]	Present Work	
397	32.5	31.4	3.3
587	36.5	34.9	4.3
704	40.6	39	3.9
852	45.7	43.8	4.1
997	49.4	47.5	3.8

Validation with numerical result

The current numerical code is used to get the surface temperature plot of the PVT module. The surface temperature plot of the PVT at the conditions of ambient temperature $T_{amb} = 34$°C, solar radiation $G = 1000$ W/m^2, inlet water temperature $T_{in} = 34$°C, and inlet fluid velocity $V_{in} = 0.0007$ m/s is compared with the figure 8(e) of Nahar et al.[45] The authors used LB250QM-60 polycrystalline silicon PV panel (1570 × 940 mm) of 5 layers, 6 × 10 number of cells, the heat exchanger (1350 × 920 × 1 mm) of aluminum metal. Cooling fluid water was passing through the heat exchanger. The authors studied the effects of inlet velocities of water and irradiation on PVT performance. The surface temperature varied from 33.99 to 125.68°C. In the current simulation, the range of the surface temperature of PVT module lies from 34 to 126°C. The comparison is displayed in Figure 4, and good matching of results is observed.

2.4.3 | Steady-state condition

In practical situation, the solar radiation and wind velocity are transient. So the operation in the case of PVT system is dynamic. When the irradiation varies, then the dynamic model is particularly appropriate to predict working temperature of solar cell as well as heat transfer

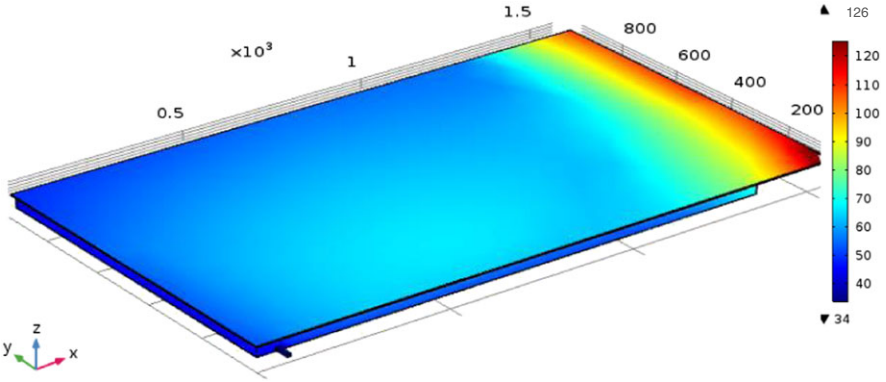

FIGURE 4 Model validation of surface temperature plot of PVT [Colour figure can be viewed at wileyonlinelibrary.com]

fluid. It is essential to produce results when steady-state condition is established for numerical simulation. In the current investigation, 3D steady state model is considered in order to avoiding the ambiguities and difficulties of time consuming 3D dynamic model. The mean temperatures of solar cell and outlet fluid against time are displayed in Figure 5. The inlet fluid temperature is 30°C, and the fluid volume flow rate is 180 L/h. From this figure, it is found that initially temperatures increase sharply. After that, the rate of change of temperatures decreases and reaches steady-state conditions. Here the steady state numerical model is found to execute as good as dynamic model.

3 | RESULTS AND DISCUSSION

Numerical simulation is performed to investigate the effect of high solar irradiance on PV cell's electrical power, thermal energy, and efficiencies in this research. The range of irradiation level is considered from 1000 to 3000 W/m^2. The volume flow rate of the working fluid is kept fixed at 180 L/h. Following sections describe the outcomes of different cases.

3.1 | Temperature of PV surface

The temperature of PV surface is displayed in Figure 6. The ambient temperature is 32°C. Initially at the lowest value of irradiation level of 1000 W/m^2, the intensity of solar irradiance is low; maximum temperature of the PV surface becomes approximately 66.7°C. Rising values of solar irradiance cause more significant thermal flow inside PV surfaces. Higher amount of heat is transferred from the PV cell to the heat exchanger for higher solar irradiation. At the highest value of solar radiation (= 3000 W/m^2), the maximum temperature of the PV surface enhances up to 134°C. This high temperature arises only at the edge points of the top surface of the PVT module.

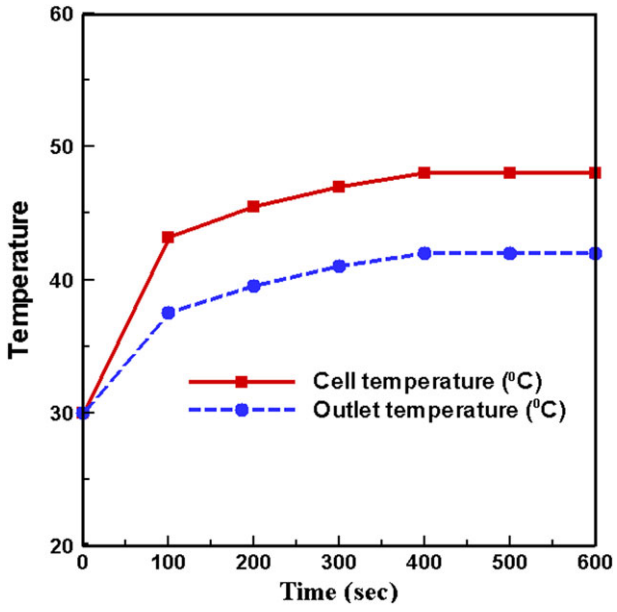

FIGURE 5 Numerical steady-state condition [Colour figure can be viewed at wileyonlinelibrary.com]

3.2 | Streamlines

The streamlines plot of the PV flowing fluid for varying solar irradiation (= 1000, 1500, 2000, 2500, and 3000 W/m^2) is displayed in Figure 7. For a graphical representation in order to visualize the streamlines properly inside the heat exchanger, the transparency is made for solid layers of the PV module. For this simulation, solar radiation G is chosen as 1000 W/m^2. Color expression for streamlines plot is given as well. The temperature of each streamline can be calculated from the temperature bar (°C). At low level of solar radiation, the fluid temperature at the outlet becomes low. This temperature of fluid increases with high irradiation level. This is significant because cooling fluid takes more heat from the heat exchanger of the PVT module at higher irradiation. This figure shows that the temperature distribution of flowing fluid from the inlet port to the outlet port changes significantly for the effect of higher irradiation. Inlet fluid mean temperature is 30°C. At the irradiation level of 1000 W/m^2, the cooling fluid temperature varies from 30°C to 42°C. This variation becomes from 30°C to 73°C for the irradiation level of 3000 W/m^2.

3.3 | PV cell temperature

Figure 8 displays the PV cell average temperature (T_{sc}) with the variation of solar radiation (G). From Equation 7, it is clear that there is a strong relation among cell temperature, ambient temperature, Tedlar temperature, and incident irradiation. Temperature of solar cell increases by 77% in the system of PV module with varying irradiation G from 1000 to 3000 W/m^2. The solar cell mean temperature is observed to be 48°C at the irradiation level of 1000 W/m^2. Mean temperature of cell becomes about 85°C at the highest irradiation of 3000 W/m^2. Bahaidarah et al[48] showed that solar cell temperature of about 1.9°C was increased for every increase of 100 W/m^2 irradiation level.

Their operating irradiation was from 240 to 979 W/m^2. Rahman et al[2] found that cell temperature of about 2.71°C was increased for each increase of irradiation level of 100 W/m^2. Their operating irradiation level was from 312 to 995 W/m^2. In the present numerical simulation, solar cell temperature T_{sc} increases by 1.85°C for the

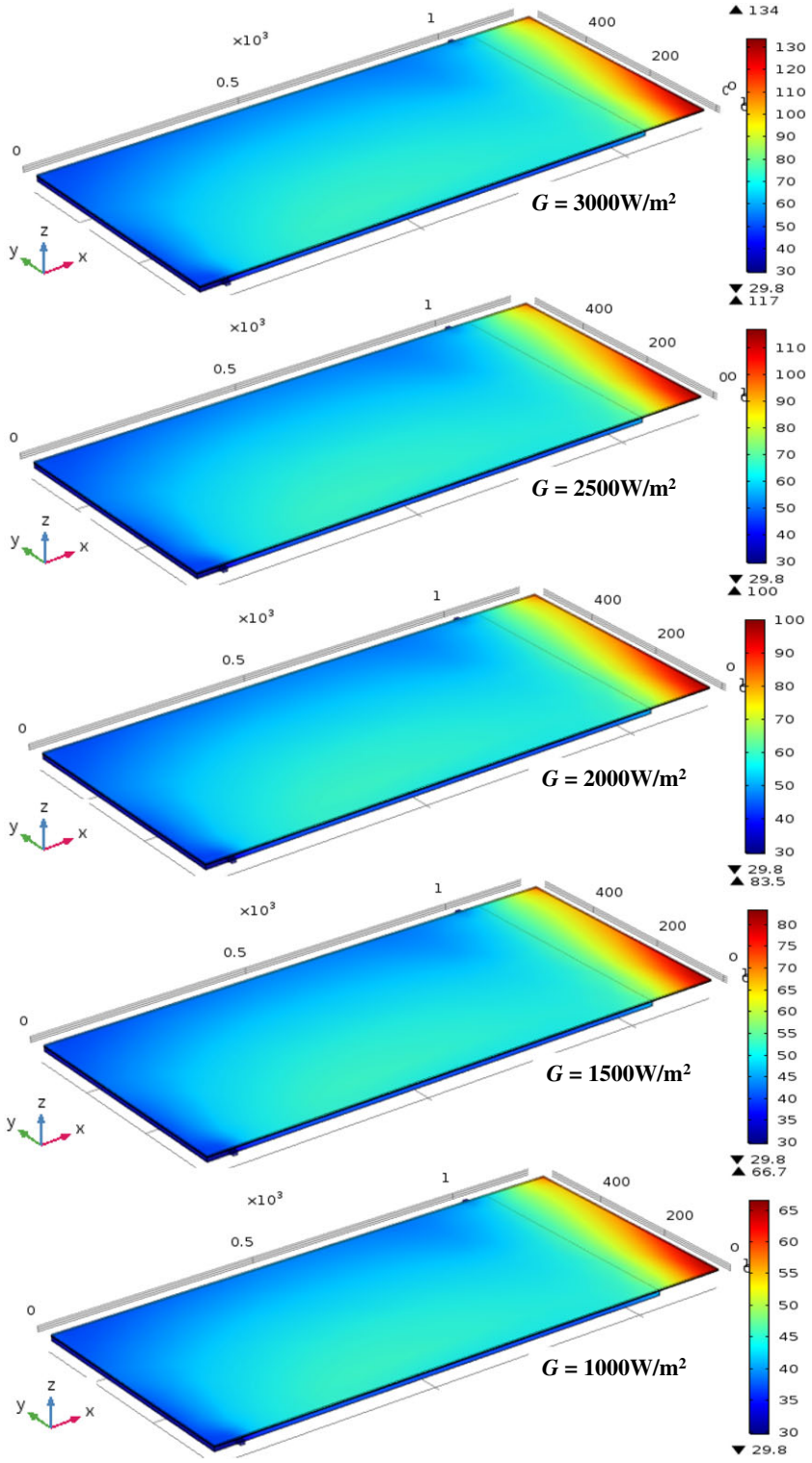

FIGURE 6 Surface temperature of the PVT module for the variation of solar radiation from 1000 to 3000 W/m^2 [Colour figure can be viewed at wileyonlinelibrary.com]

increment of each 100-W/m^2 solar irradiance. This agrees well with the results of Rahman et al[2] and Bahaidarah et al.[48]

3.4 | Electrical power and energy

Figure 9A,B displays the total amount of producing electrical power E in both watt and kilowatt hour units for different irradiation G (1000–3000 W/m^2) by using Equation 14. Output electrical power increases linearly with the increasing value of irradiation. This is because higher irradiation enhances current and voltage inside the PV. Generally, the rate of current increment is linear whereas that of voltage is logarithmic. The increasing rate of current is much higher than that of voltage. At 1000 W/m^2 irradiation, produced cell energy is

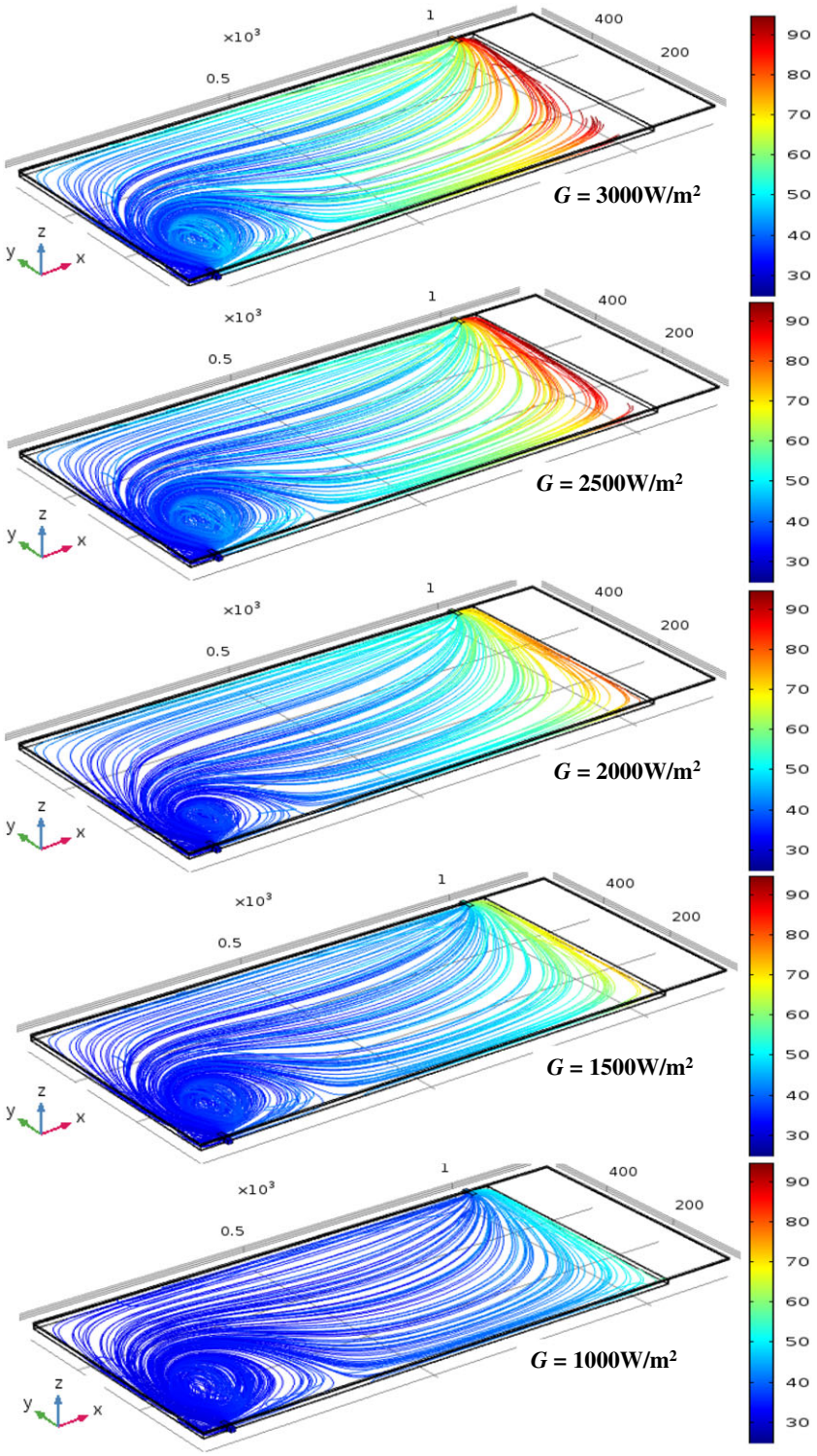

FIGURE 7 Streamline plots of fluid flow for the variation of solar radiation from 1000 to 3000 W/m^2 [Colour figure can be viewed at wileyonlinelibrary.com]

63 W, and at 3000 W/m^2 irradiation, it becomes approximately 190 W. Approximately 127 W electrical power is increased for 2000-W/m^2 increment of irradiation. Thus, produced electrical power enhances by 6.4 W for each increment of irradiation of 100 W/m^2 for PV cell. Rahman et al[2] found that for PV module without cooling system, an increase of 3.88 W in output power was found for each increase of 100 W/m^2 irradiation. The present numerical result differs with Rahman et al[2] because of the fluid velocity, poor installation, and operating conditions.

For the city Kuala Lumpur of Malaysia, the daily average sunny hour is assumed to be 4 hours. Then for a single sunny day, the total amount of produced electrical energy is about 0.8 kWh by PV cell at the value of irradiation 3000 W/m^2.

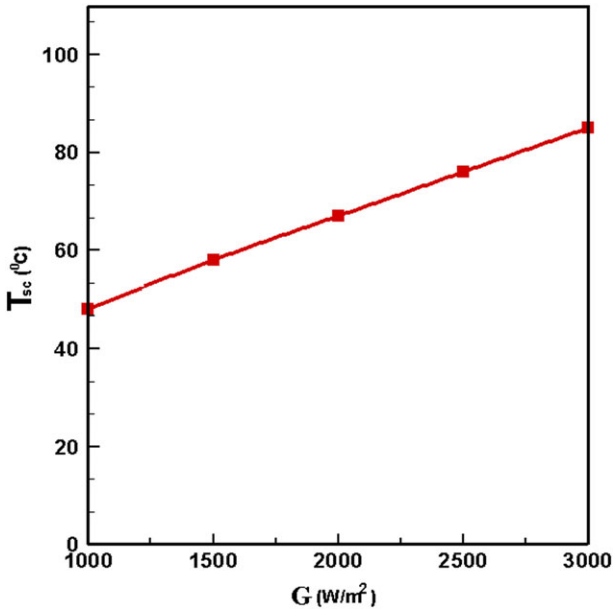

FIGURE 8 PV cell temperature versus solar radiation [Colour figure can be viewed at wileyonlinelibrary.com]

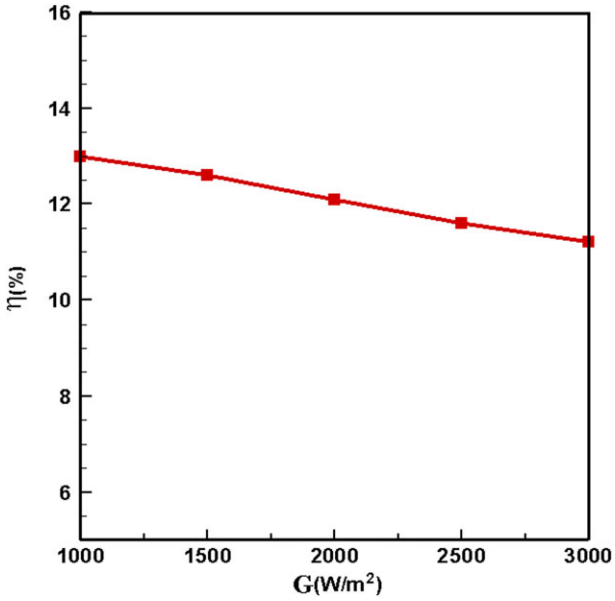

FIGURE 10 Electrical efficiency with the variation of irradiation [Colour figure can be viewed at wileyonlinelibrary.com]

3.5 | Electrical efficiency

Figure 10 shows the percentage of the PV module's electrical efficiency against the solar radiation (from 1000 to 3000 W/m^2). Increasing irradiation (G) decreases the electrical efficiency of the module. The decrement of electrical efficiency is found from 13% to 11.2% in the PV cell with increasing values of irradiation. This result agrees with the formula of electrical efficiency given in Equation 16. For each 100-W/m^2 increase in irradiation, cell efficiency decreases by 0.09%. The authors[45] found that the electrical efficiency decreased by about 0.16% for each increase of irradiation 100 W/m^2. Thus, present numerical result agrees with their result very well.

3.6 | Outlet fluid temperature

Fluid outlet mean temperature, T_{out} (°C), is expressed in Figure 11 for the variation of solar irradiance (1000−3000 W/m^2) with volume flow rate of 180 L/h. Inflow fluid mean temperature is 30°C. Fluid outlet temperature increases because of increasing values of irradiation. The outlet fluid mean temperature is observed to be 42°C at the irradiation level of 1000 W/m^2. For the highest irradiation of 3000 W/m^2, the mean output temperature is 73°C. Thus, outlet fluid average temperature increases by 1.55°C for each increment of 100 W/m^2 solar radiation. This hot water can be used in many purposes.

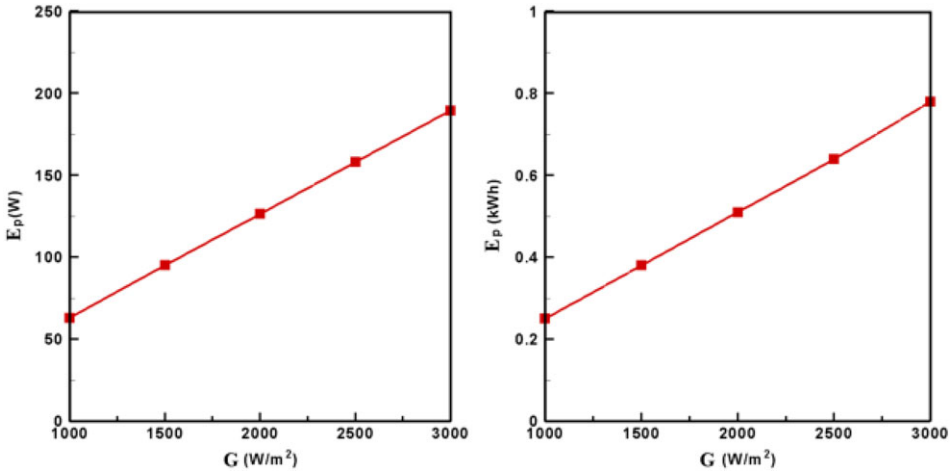

FIGURE 9 Electrical (A) power and (B) energy with the variation of irradiation [Colour figure can be viewed at wileyonlinelibrary.com]

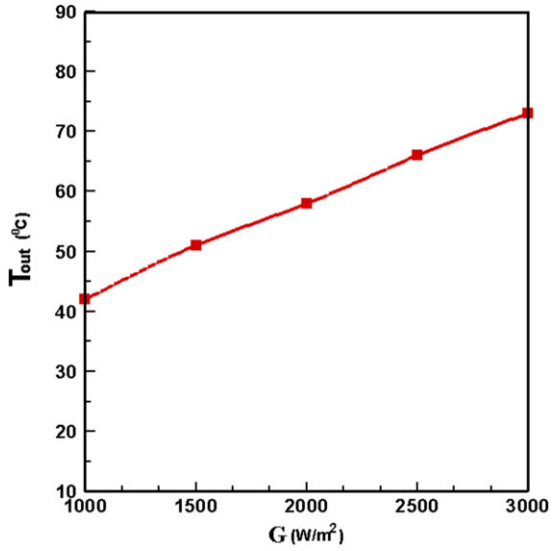

FIGURE 11 Outlet fluid temperature with the variation of irradiation [Colour figure can be viewed at wileyonlinelibrary.com]

3.7 | Thermal energy

The amount of total output thermal energy can be calculated for the PVT cooling system using Equation 15. Extracted thermal energy from the PVT system for the variation of solar radiation is expressed in Figure 12. At the 1000-W/m^2 irradiation level, the extracted thermal power in the PVT module is 362 W. The value of this power becomes 988 W for the irradiation level of 3000 W/m^2 at the fixed volume flow rate 180 L/h. This is happening because of conduction and convection heat flow from the PV to the heat exchanger and from the heat exchanger to the cooling fluid, respectively. As a result, higher temperature difference occurs between outlet and inlet fluid for higher irradiation. Figure 12 shows that an increment of 31.3 W thermal energy can be extracted from the system for each 100-W/m^2 increase of irradiation.

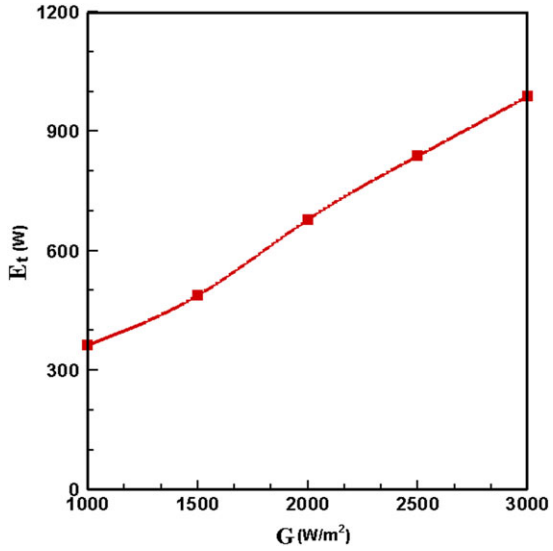

FIGURE 12 Thermal energy with the variation of irradiation [Colour figure can be viewed at wileyonlinelibrary.com]

3.8 | Thermal efficiency

Figure 13 shows that at the fixed volume flow rate of 180 L/h, the thermal efficiency decreases with increasing solar radiation level (1000, 1500, 2000, 2500, and 3000 W/m^2). Thermal efficiency is measured using Equation 17. As the total received energy, E_{in} (W), increases for the escalating values of irradiation, the thermal efficiency decreases. It is logical and proved by Equations 2 and 17. Thermal efficiency decreases from 74% to 68% for the variation of irradiation. Approximately 0.3% decrement of thermal efficiency is observed for each 100-W/m^2 increase of solar radiation.

3.9 | Overall efficiency

Figure 14 depicts the overall efficiency graph of the PVT module against solar radiation. Using Equation 18, overall efficiency of the PVT is calculated. Overall efficiency drops from 87% to 79.2% with increasing values of irradiation from 1000 to 3000 W/m^2 at 180 L/h volume flow rate. Thus, 7.9% overall efficiency decreases for the increase of 2000 W/m^2 irradiation. Overall efficiency decreases about 0.39% for each 100-W/m^2 increase of irradiation level.

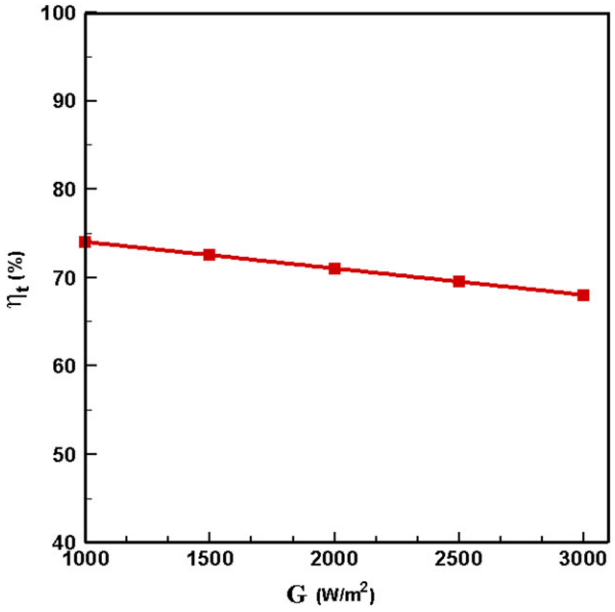

FIGURE 13 Thermal efficiency with the variation of irradiation [Colour figure can be viewed at wileyonlinelibrary.com]

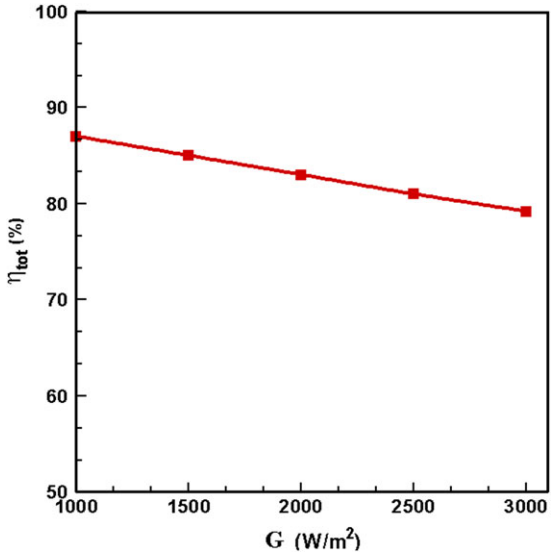

FIGURE 14 Overall efficiency with the variation of irradiation [Colour figure can be viewed at wileyonlinelibrary.com]

3.10 | Cell temperature effect

The cell temperature affects the electrical power and efficiency. This is shown in Figure 15A,B with the variation of irradiation (G = 1000–3000 W/m^2). Electrical power and efficiency decrease with the rising values of solar cell temperature at a fixed irradiation level. This satisfies Equations 14 and 16. In the present numerical study for the PV module at G = 1000 W/m^2, the module output energy is 63 W, the efficiency is 13%, and the cell temperature is 48°C. If cell temperature is increased up to 60°C, then output power and efficiency decrease to 50.9 W and 12.2%, respectively. Thus, total output energy and efficiency decrease to 12.1 W and 0.8%, respectively, with increasing cell temperature from 48°C to 60°C. For each 1°C increment of solar cell temperature, electrical energy and efficiency decrease to 1.0 W and 0.06%, respectively.

3.11 | Comparison

3.11.1 | Efficiency

The electrical efficiency reduction for each increase of 1°C cell temperature (T_{sc}) that is the result from different investigations of Nahar et al,[45] Bahaidarah et al,[48] Chandrasekar et al,[49] and present research is shown in Table 6. The authors[45] showed that the electrical power and efficiency decreased about 1.7 W and 0.13%,

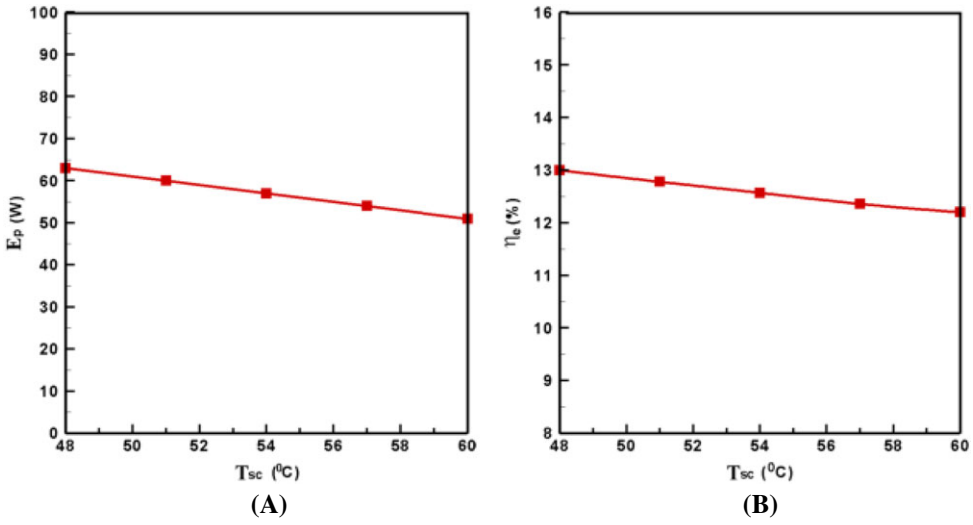

FIGURE 15 A, Power against cell temperature. B, Efficiency against cell temperature [Colour figure can be viewed at wileyonlinelibrary.com]

TABLE 6 Reduction of cell temperature of each 1°C

Different investigations	G (W/m^2)		T_{sc} (°C)		T_{amb} (°C)	Efficiency		Efficiency Reduction (%) per 1°C Cell Temperature Increment
	Initial	Final	Initial	Final		Initial	Final	
[45]	1000	1000	60.5	66	34	10	9.3	0.13
[48]	240	979	25	44	21	15.7	15.2	0.03
[49]	600	1300	37	65	37	10.3	9	0.05
Present research	1000	1000	48	60	32	13	12.2	0.06

respectively, for each increase of 1°C cell temperature. On the other hand, the researchers of Bahaidarah et al[48] and Chandrasekar et al[49] found decreasing trend of electrical efficiency about 0.05% and 0.03% for each 1°C increment of cell temperature, respectively. The current numerical result agrees perfectly with Nahar et al.[45] A slight difference is observed with Nahar et al[45] and Chandrasekar et al[49] because of different operating conditions. So in order to get more electrical power and efficiency, the solar cell temperature (T_{sc}) has not to be increased after a certain level. Solar cell temperature is inversely related to the electrical efficiency of PV module. Table 6 displays the efficiency reduction percentage for the increment of each 1°C cell temperature.

3.11.2 | Cell temperature

Table 7 displays the comparison of the increment in cell temperature (T_{sc}) for every 100-W/m^2 increment in solar irradiance (G) that is the result from different investigations, namely Teo et al,[1] Rahman et al,[2] Bahaidarah et al,[48] Chandrasekar et al,[49] and the current work. The result of the present investigation of PV module differs from Rahman et al[2] and agrees fine with that of Teo et al,[1] Bahaidarah et al,[48] and Chandrasekar et al.[49]. The current numerical investigation is conducted with constant irradiation variation, reference temperature, sky temperature, ambient temperature, etc.

3.11.3 | Regression equation

Using analysis of regression, a linear equation is obtained for PV module's electrical efficiency (η) and solar cell temperature (T_{sc}). In the present numerical regression equation, the confidence coefficient is $r^2 = 0.9802$. Table 8 shows the comparison for linear regression equations between present numerical work and Chandrasekar et al.[49] They used PV module with cooling system where the temperature coefficient was 0.0083 (%/°C). From Table 8, it is seen that good agreement is found between these 2 results. At the solar cell temperature of 50°C, the computed error between present numerical result and that of Chandrasekar et al[49] is also shown in this table.

3.12 | Correlation

Equation 1 shows the correlation of T_{sc} with G from experimental data for low irradiation (up to 1000 W/m^2). Now, a correlation is developed from the result of numerical simulation for high irradiation (1000–3000 W/m^2). This is written as

$$T_{sc} = 1.3325^{*}(G)^{0.5172} \text{ where the correlation coefficient is } r^2 = 0.9969. \quad (19)$$

Equation 19 is in a similar pattern of Equation 1. This shows the demonstration of numerical validity. The

TABLE 7 Increment of PV temperature per 100 W/m^2 irradiation

Different investigations	Irradiation (W/m^2)		Operating temperature (°C)		Cell temperature increment per 100 W/m^2 irradiation	Ambient temperature (°C)
	Initial	Final	Initial	Final		
[1]	550	1050	41	48	1.4	
[2]	312	995	31	50	2.71	35
[48]	240	979	21	35	1.9	21
[49]	600	1300	40	50	1.4	37
Present research	1000	3000	48	85	1.85	32

TABLE 8 Comparison of linear regression equations

Investigations	G (W/m^2)		T_{sc} (°C)		Regression Equation	Efficiency at 40°C Cell Temperature	Error (%)
	Initial	Final	Initial	Final			
Chandrasekar et al[49]	600	1300	40	50	$\eta = 0.177 - 0015 \times T_{sc}$	10.2	4.9
Present numerical work	1000	3000	48	85	$\eta = 0.151 - 0.000\,88 \times T_{sc}$	10.7	

TABLE 9 Comparison between experimental and numerical regression equations

Description of Investigation	Regression Equation	Cell Temperature (°C) at 1000 W/m^2 Irradiation	Percentage of Error (%)
Experimental	$T_{sc} = 2.4128 \times (G)^{0.4363}$	49.11	3.3
Numerical work	$T_{sc} = 1.3325 \times (G)^{0.5172}$	47.45	

percentage of error between these 2 correlations for solar cell temperature at irradiation of 1000 W/m^2 is shown in Table 9.

4 | CONCLUSION

The effect of high solar radiation on PV module performance has been investigated numerically. Temperature distribution throughout the PV module and velocity distribution of cooling fluid inside the heat exchanger because of the variation of irradiation from 1000 to 3000 W/m^2 have been described. In addition, solar cell temperature, generated electrical power and efficiency, extracted thermal energy and efficiency, and overall efficiency have been evaluated. Main findings from the present research can be written as follows:

- At the 1000 W/m^2 irradiation, the electrical power and efficiency increase by 1.0 W and 0.06% for each 1°C decrease in cell temperature.
- The electrical power and thermal energy increase by about 6.4 and 31.3 W for every 100-W/m^2 increase in irradiation level.
- Electrical power and thermal energy enhance by approximately 201.6% and 175.14%, respectively, because of the variation of irradiation level of 1000 to 3000 W/m^2.
- Output fluid temperature increases by about 1.55°C for each 100-W/m^2 increase in irradiation.
- Overall energy increases by about 1797.06% with increasing irradiation from 1000 to 3000 W/m^2.

Thus, high irradiation increases electrical power and thermal energy of the PVT system. A large power plant with this new developed model can effectively meet the domestic energy demand in the future.

ACKNOWLEDGEMENT

The research has been conducted by the financial support from UMPEDAC, HICoE grant, Ministry of Higher Education (project: UM.0000067/HME.OM, UMPEDAC-2016).

ORCID

R. Nasrin http://orcid.org/0000-0002-5032-4287

REFERENCES

1. Teo HG, Lee PS, Hawlader MNA. An active cooling system for photovoltaic modules. *Appl Energy*. 2012;90(1):309-315.
2. Rahman MM, Hasanuzzamana M, Rahim NA. Effects of operational conditions on the energy efficiency of photovoltaic modules operating in Malaysia. *J of Cleaner Production*. 2017;143:912-924.
3. Koech RK, Ondieki HO, Tonui JK, Rotich SK. A steady state thermal model for photovoltaic/thermal (PV/T) system under various conditions. *Int J of Sci & Tech Res*. 2012;1:11
4. Chow TT. A review on photovoltaic/thermal hybrid solar technology. *Appl Energy*. 2010;87:365-379.
5. Ibrahim A, Othman MY, Ruslan MH, et al. Performance of photovoltaic thermal collector (PVT) with different absorbers design. *WSEAS Trans on Environ and Develop*. 2009;5(3):321-330.
6. Jin GL, Ibrahim A, Chean YK, et al. Evaluation of single-pass photovoltaic-thermal air collector with rectangle tunnel absorber. *Amer J of Appl Sci*. 2010;2:277-282.
7. Nasrin R, Alim MA, Chamkha AJ. Effects of physical parameters on natural convection in a solar collector filled with nanofluid. *Heat Trans-Asian Res*. 2013;42(1):73-88.
8. Nasrin R, Alim MA. Semi-empirical relation for forced convective analysis through a solar collector. *Solar Energy*. 2014;105:455-467.
9. Nasrin R, Parvin S, Alim MA. Heat transfer and collector efficiency through direct absorption solar collector with radiative heat flux effect. *Num Heat Trans Part A- Application*. 2015;68:1-21.
10. Hasanuzzaman M, Al-Amin AQ, Khanam S, Hosenuzzaman M. Photovoltaic power generation and its economic and environmental future in Bangladesh. *J of Renew and Sust Energy*. 2015;7(1): 013108
11. Hosenuzzaman M, Rahim NA, Selvaraj J, Hasanuzzaman M, Malek ABMA, Nahar A. Global prospects, progress, policies, and environmental impact of solar photovoltaic power generation. *Renew. and Sust. Energy Rev*. 2015;41:284-297.
12. Ahmed F, Al Amin AQ, Hasanuzzaman M, Saidur R. Alternative energy resources in Bangladesh and future prospect. *Renew and Sust Energy Rev*. 2013;25:698-707.
13. Tiwari A, Sodha MS. Parametric study of various configurations of hybrid PV/thermal air collector: experimental validation of theoretical model. *Solar Energy Mat & Solar Cells*. 2007;91:17-28.
14. Joshi AS, Tiwari A, Tiwari GN, Dincer I, Reddy BV. Performance evaluation of a hybrid photovoltaic thermal (PV/T) (glass-to-glass) system. *Int J Therm Sci*. 2009;48:154-164.
15. Sarhaddi F, Farahat S, Ajam H, Behzadmehr A, Adeli MM. An improved thermal and electrical model for a solar photovoltaic thermal (PV/T) air collector. *Appl Energy*. 2010;87:2328-2339.
16. Riffat SB, Cuce E. A review on hybrid photovoltaic/thermal collectors and systems. *Int J Low-Carbon Tech*. 2011. https://doi.org/10.1093/ijlct/ctr016; July 21
17. Vokas G, Christandonis N, Skittides F. Hybrid photovoltaic thermal systems for domestic heating and cooling—a theoretical approach. *Solar Energy*. 2006;80:607-615.
18. Ronak D, Adnan I, Goh LJ, Ruslan MH, Kamaruzzaman S. Predicting the performance of amorphous and crystalline silicon based photovoltaic solar thermal collectors. *Energy Conv. and Manag*. 2011;52:1741-1747.
19. Adiyabat A, Kurokawa K, Otani K, et al. Evaluation of solar energy potential and PV module performance in the Gobi Desert of Mongolia. *Prog in Photovoltaics: Res and Appl*. 2006;14:553-566.

20. Makrides G, Zinsser B, Phinikarides A, Schubert M, Georghiou GE. Temperature and thermal annealing effects on different photovoltaic technologies. *Renew Energy*. 2012;43:407-417.
21. Lim JL, Woo SC, Jung TH, Min YK, Won CS, Ahn HK. Analysis of factor on the temperature effect on the output of PV module. *Trans of the Korean Inst of Electrical Engineers*. 2013;62:365-370.
22. Skoplaki E, Palyvos JA. On the temperature dependence of photovoltaic module electrical performance: a review of efficiency/power correlations. *Solar Energy*. 2009;83:614-624.
23. Makrides G, Bastian Z, George EG, Markus S, Jurgen HW. Temperature behaviour of different photovoltaic systems installed in Cyprus and Germany. *Solar Energy Mat. and Solar Cells*. 2009;93:1095-1099.
24. Saxena N, Singh B, Vyas AL. Single-phase solar PV system with battery and exchange of power in grid-connected and standalone models. *IET Renew. Power Gen.* 2017;11(2):325-333.
25. Belkaid A, Gaubert JP, Gherbi A. Design and implementation of a high-performance technique for tracking PV peak power. *IET Renew Power Gen*. 2017;11(1):92-99.
26. Kalogirou SA, Tripanagnostopoulos Y. Hybrid PV/T solar systems for domestic hot water and electricity production. *Energy Conv and Manag*. 2006;47:3368-3382.
27. Nishioka K, Hatayama T, Uraoka Y, Fuyuki T, Hagihara R, Watanabe M. Field-test analysis of PV system output characteristics focusing on module temperature. *Solar Energy Mat and Solar Cells*. 2003;75:665-671.
28. Tiwari A, Barnwal P, Sandhu GS, Sodha MS. Energy metrics analysis of hybrid photovoltaic (PV) modules. *Appl Energy*. 2009;86:2615-2625.
29. Tiwari GN, Mishra RK, Solanki SC. Photovoltaic modules and their applications: a review on thermal modeling. *Appl Energy*. 2011;88:2287-2304.
30. Van Dyk EE, Scott BJ, Meyer EL, Leitch AWR. Temperature dependence of performance of crystalline silicon modules. *S Afr J Sci*. 2000;96:198-200.
31. El –Sayed SM, Anis WR, Hafez IM. The effect of temperature on the performance of PV array operating under concentration. *Int. J. of Sci. & Tech. Res.* 2015;4(8):240-246.
32. Avireni S., Converging lens solar concentrator and their position controlled using a microprocessor for increasing the efficiency of solar photovoltaic energy conversion, 3rd Int. Conf.: Sci. of Elect., Techn. of Inf. and Tel., 2005; March 27–31: Tunisia.
33. Xie WT, Dai YJ, Wang RZ, Sumathy K. Concentrated solar energy applications using Fresnel lenses: a review. *Renew Sustain Energy Rev*. 2011;15:2588-2606.
34. Kasaeian A, Khanjari Y, Golzari S, Mahian O, Wongwises S. Effects of forced convection on the performance of a photovoltaic thermal system: an experimental study. *Exp Thermal and Fluid Sci*. 2017;85:13-21.
35. Kianifar A, Heris SZ, Mahian O. Exergy and economic analysis of a pyramid-shaped solar water purification system: active and passive cases. *Energy*. 2012;38:31-36.
36. Sabiha MA, Saidur R, Mekhilef S, Mahian O. Progress and latest developments of evacuated tube solar collectors. *Renew. and Sust. Energy Rev.* 2015;51:1038-1054.
37. Mahian O, Kianifar A, Kalogirou SA, Pop I, Wongwises S. A review of the applications of nanofluids in solar energy, Int. *J of Heat and Mass Trans*. 2013;57:582-594.
38. Meibodi SS, Kianifar A, Niazmand H, Mahian O, Wongwises S. Experimental investigation on the thermal efficiency and performance characteristics of a flat plate solar collector using SiO_2/EG–water nanofluids. *Int Commun in Heat and Mass Trans*. 2015;65:71-75.
39. Mahian O, Kianifar A, Heris SZ, Wongwises S. First and second laws analysis of a minichannel-based solar collector using boehmite alumina nanofluids: effects of nanoparticle shape and tube materials, Int. *J. of Heat and Mass Trans.* 2014;78:1166-1176.
40. Mahian O, Kianifar A, Heris SZ, Sahin AZ, Wen D, Wongwises S. Nanofluids effects on the evaporation rate in a solar still equipped with a heat exchanger. *Nano Energy*. 2017;36:134-155.
41. Schepper ED, Passel SV, Lizin S. Economic benefits of combining clean energy technologies: the case of solar photovoltaics and battery electric vehicles. *Int J of Energy Res*. 2015;39(8):1109-1119.
42. He Y, Xiao L, Li L. Research on the influence of PV cell to thermal characteristics of photovoltaic/thermal solar system. *Int. J. of Energy Res.* 2017;41(9):1287-1294.
43. Sathya P, Natarajan R. Numerical simulation and performance measure of highly efficient GaP/InP/Si multi-junction solar cell. *Int. J. of Energy Res.* 2017;41(8):1211-1222.
44. Du Y, Le NCH, Chen D, Chen H, Zhu Y. Thermal management of solar cells using a nano-coated heat pipe plate: an indoor experimental study. *Int. J. of Energy Res.* 2017;41(6):867-876.
45. Nahar A, Hasanuzzaman M, Rahim NA. Numerical and experimental investigation on the performance of a photovoltaic thermal collector with parallel plate flow channel under different operating conditions in Malaysia. *Solar Energy*. 2017;144:517-528.
46. Reddy JN, Gartling DK. *The Finite Element Method in Heat Transfer and Fluid Dynamics*. Boca Raton, FL: CRC Press, Inc.; 1994.
47. Nasrin R, Alim MA. Laminar free and forced magnetoconvection through an octagonal channel with a heat generating circular cylinder. *J of Naval Arch and Marine Engg*. 2012;9(1):25-34.
48. Bahaidarah H, Subhan A, Gandhidasan P, Rehman S. Performance evaluation of a PV (photovoltaic) module by back surface water cooling for hot climatic conditions. *Energy*. 2013;59:445-453.
49. Chandrasekar M, Suresh S, Senthilkumar T, Karthikeyan MG. Passive cooling of standalone flat PV module with cotton wick structures. *Energy Conv. and Manag.* 2013;71:43-50.

How to cite this article: Nasrin R, Hasanuzzaman M, Rahim NA. Effect of high irradiation on photovoltaic power and energy. *Int J Energy Res*. 2018;42:1115–1131. https://doi.org/10.1002/er.3907